Heliyon 9 (2023) e17402

Contents lists available at ScienceDirect

Heliyon

journal homepage: www.cell.com/heliyon

Measurement and correlation of solubility data for deferiprone in propylene glycol and 2-propanol at different temperatures

Homa Rezaei [a,b], Elaheh Rahimpour [b,c,*], Fleming Martinez [d], Abolghasem Jouyban [b,e]

[a] Student Research Committee, Faculty of Pharmacy, Tabriz University of Medical Sciences, Tabriz, Iran
[b] Pharmaceutical Analysis Research Center and Faculty of Pharmacy, Tabriz University of Medical Sciences, Tabriz, Iran
[c] Infectious and Tropical Diseases Research Center, Tabriz University of Medical Sciences, Tabriz, Iran
[d] Grupo de Investigaciones Farmacéutico-Fisicoquímicas, Departamento de Farmacia, Universidad Nacional de Colombia, Sede Bogotá, Cra. 30 No. 45-03, Bogotá D. C., Colombia
[e] Pharmaceutical Sciences Research Center, Shahid Beheshti University of Medical Sciences, Tehran, Iran

ARTICLE INFO

Keywords:
solubility
Deferiprone
Binary solvent mixtures
Cosolvency models
Thermodynamics

ABSTRACT

This investigation dealt with the thermodynamic properties, saturated solubility values, and solvation behavior of deferiprone as an oral iron chelator agent in non-aqueous mixtures of propylene glycol and 2-propanol using experimental measurements and mathematical correlations. The solubility of deferiprone demonstrated a positive correlation with both temperature and propylene glycol mass fraction. Four mathematical models were employed to correlate the solid-liquid equilibrium data, and the low mean relative deviation values of less than 3.6% illustrate the good agreement of computed data with the experimental data. The apparent thermodynamic behavior of deferiprone dissolution was also investigated according to van't Hoff and Gibbs equation.

1. Introduction

Patients who are diagnosed with congenital hemolytic anemia like hereditary spherocytosis, sickle cell anemia, and thalassemia are required to receive regular packed red blood cells via parenteral transfusion from the early ages to diminish the severity of clinical manifestations of organomegaly and to keep possession of optimal growth [1,2]. This type of treatment is considered a lifelong necessity unless stem cell transplantation or splenectomy (in the case of hereditary spherocytosis) is undertaken. As a result, transfusion-induced iron overload has become a severe challenge and complication for patients and healthcare professionals [3]. Deferiprone (3-hydroxy-1,2-dimethylpyridin-4(1H)-one, Fig. 1) is an orally active iron chelator and is considered the drug of choice in thalassemia patients who are exposed to iron overload [4,5]. Deferiprone has traditionally been administered in the form of tablets; however, deferiprone liquid formulation has recently been launched in the pharmaceutical market to ease the taking of this medication in children younger than 10 years and those with difficulties swallowing tablets [6]. Oral administration is the most preferred and the most convenient route of drug administration. However, this delivery route is so complicated based on physiological factors like gastric emptying rate, blood flow, pH, and composition of alimentary secretions that would influence the extent and/or rate of drug absorption. For the *in vitro* assessment of *in vivo* behavior of a drug formulation, the solubility and/or dissolution tests are commonly

* Corresponding author. Pharmaceutical Analysis Research Center and Faculty of Pharmacy, Tabriz University of Medical Sciences, Tabriz, Iran.
E-mail address: rahimpour_e@yahoo.com (E. Rahimpour).

https://doi.org/10.1016/j.heliyon.2023.e17402
Received 24 April 2023; Received in revised form 15 June 2023; Accepted 15 June 2023
Available online 19 June 2023

applied for development purposes and quality control [7]. Drug solubility determination in an aqueous medium plays a crucial role in drug discovery and pre-formulation studies. So that the aqueous solubility and dissolution essentially influence the fraction of substance absorbed from the intestine, as well as oral bioavailability [8,9]. However, experimental tests are a tedious and time-consuming process. As a result, any alternative techniques, including predictive mathematical models, could be noteworthy tools for pharmaceutical specialists. Most of these models are well compared [10] and reviewed [11] in our previous works. Recently, deferiprone solubility in the aqueous binary mixtures of ethylene glycol, propylene glycol, polyethylene glycol 400 [12], ethanol, *N*-methyl-2--pyrrolidone [13], and some mono-solvents such as chloroform, 1,4-dioxane, ethyl acetate, acetonitrile, and dichloromethane [14] has been determined. In continuation of the previous works, this study aimed to (i) report the experimental solubility data and density values of deferiprone in the non-aqueous binary mixtures of propylene glycol and 2-propanol at various temperatures; (ii) fit the experimental solubility data by some mathematical cosolvency models; (iii) calculate the thermodynamic parameters of deferiprone in neat and binary solvents using the Gibbs and van't Hoff equations, and (iv) evaluate the effect of Lewis acid-base, polarizability and cavity effects on the deferiprone solubility in these mixtures.

2. Materials and method

2.1. Materials

Ample descriptions of deferiprone and selected solvents are depicted in Table 1. Deferiprone had a purity achieved up to 0.997 via HPLC and was purchased from Arasto Pharmaceutical Chemicals Inc (Tehran, Iran). All organic solvents, including ethanol, propylene glycol, and 2-propanol, were of analytical grade and employed without further purification. Double distilled water was prepared in the laboratory.

2.2. Measurement of deferiprone solubility

The solubility data of deferiprone in the non-aqueous binary systems of propylene glycol and 2-propanol was measured by the shake-flask method [15] at 101.3 kPa. For each experiment, binary solvent non-aqueous mixtures of propylene glycol and 2-propanol were prepared at several mass fractions ranging from 0.0 to 1.0 at intervals of 0.1. Mixed solvents were prepared in glass vials by weighing neat solvents (propylene glycol and 2-propanol) by a predetermined mass fraction. Excess deferiprone powder was dispersed into glass vials containing the non-aqueous binary mixtures. Afterward, glass vials were sealed to keep our solvents from evaporating and then transferred on a shaker (Behdad, Tehran, Iran) into an incubator (Kimia Idea Pardaz Azerbaijan, Tabriz, Iran) and continuously stirred at temperatures ranging from 293.2 to 313.2 K. After 48 h, if the solid powder was not completely vanished, the solid-liquid mixtures can be judged to be saturated at that specific point. The dissolution rate experiments confirmed that the shaking time was sufficient. The shaker was stopped, and the solutions were kept to sediment the insoluble powder. A centrifuge completely separated the solid powder from the liquid phase. A portion of supernatant was carefully taken out from the saturated solution, using a sampler, and diluted with ethanol: water (30:70). A UV–vis spectrophotometer (Cecil BioAquarius CE 7250, UK) was employed to detect the concentration at 273.5 nm. It should be noted that the absorbance of diluted solutions should be within the predetermined calibration curve to ensure the accuracy of the obtained data. To better assess the solubility, each experiment was carried out at least three times and the estimated uncertainty of the solubility values was less than 10%. The densities of the saturated solutions were also measured using a 5 mL pycnometer with an uncertainty of 0.001 g cm^{-3}.

2.3. Computational section

Four different computational models (van't Hoff, mixture response surface (MRS), Jouyban-Acree, and Jouyban-Acree-van't Hoff) were applied to the mathematical representation of the experimental deferiprone solubility values. These models are widely applied in the field of solubility prediction and model regression can be obtained by computer programming. The details of each model are given in the following sections. Calculation of mean relative deviation (*MRD*%) can evaluate the accuracy of cosolvency models. It is

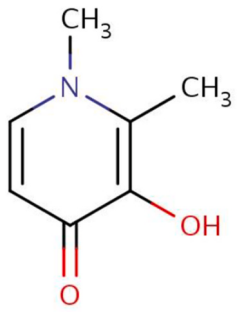

Fig. 1. Molecular structure of deferiprone.

Table 1
Details of the materials specification.

Chemical Name	CAS No.	Molecular formula	Molar mass ($g \cdot mol^{-1}$)	Source	Purity (percentage)	Analysis method
Deferiprone	30652-11-0	$C_7H_9NO_2$	139.15	Arasto Pharmaceutical Chemicals Inc	≥ 99.7%	HPLC[a]
2-Propanol	67-63-0	C_3H_8O	60.10	Merck	≥ 99.8%	GC[b]
Propylene glycol	57-55-6	$C_3H_8O_2$	76.09	Merck	≥ 99.5%	GC[b]
Distilled deionized water	7732-18-5	H_2O	18.02	Shahid Ghazi Pharmaceutical Co.	≥ 99.9%	GC[b]
Ethanol	64-17-5	C_2H_6O	46.07	Jahan Alcohol Teb	≥ 93.5%	GC[b]

[a] High-performance liquid chromatography.
[b] Gas chromatography.

calculated as Eq. (1):

$$MRD\% = \frac{100}{N}\sum\left(\frac{|Calculated\ Value - Observed\ Value|}{Observed\ Value}\right) \quad (1)$$

where N demonstrates the number of data points. The statistical analysis was performed by SPSS software version 16.0 (SPSS Inc., Chicago, IL, USA).

2.3.1. van't Hoff equation

The van't Hoff equation depicts the linear relationship between the reciprocal of the solution's absolute temperature and the logarithm of the solute mole fraction. The model expression is manifest as Eq. (2) [16]:

$$\ln x = A + \frac{B}{T} \quad (2)$$

where A and B are defined as the model parameters.

2.3.2. The Jouyban-Acree model

The Jouyban-Acree model, which demonstrates the relationship between the solute solubility with temperature and solvent composition, is written as Eq. (3) [17]:

$$\ln x_{m,T} = w_1 \ln x_{1,T} + w_2 \ln x_{2,T} + \frac{w_1.w_2}{T}\sum_{i=0}^{2} J_i.(w_1 - w_2)^i \quad (3)$$

in which $x_{1,T}$ and $x_{2,T}$ are the solubility value in mono-solvents at a temperature of T, w_1 and w_2 are the mass ratios of solvents 1 and 2 in the absence of solute, and J_i terms are the model parameters achieved by linear regression of $(\ln x_{m,T} - w_1 \ln x_{1,T} - w_2 \ln x_{2,T})$ against $\frac{w_1.w_2}{T}$, $\frac{w_1.w_2(w_1-w_2)}{T}$, and $\frac{w_1.w_2(w_1-w_2)^2}{T}$.

2.3.3. The Jouyban-Acree-van't Hoff model

A combination of the van't Hoff equation and the Jouyban-Acree model generates an accurate model for the correlation and/or estimation of solute solubility data in the investigated mixtures. The Jouyban-Acree-van't Hoff model can be presented as Eq. (4) [17]:

$$\ln x_{m,T} = w_1\left(A_1 + \frac{B_1}{T}\right) + w_2\left(A_2 + \frac{B_2}{T}\right) + \frac{w_1.w_2}{T}\sum_{i=0}^{2} J_i.(w_1 - w_2)^i \quad (4)$$

where A_1, B_1, A_2 and B_2 are the van't Hoff model's constants obtained by plotting $\ln x_{m,T}$ against $1/T$ in the mono-solvents at various temperatures. J_i terms are computed using linear regression of $\left(\ln x_{m,T} - w_1\left(A_1 + \frac{B_1}{T}\right) - w_2\left(A_2 + \frac{B_2}{T}\right)\right)$ *vs.* $\frac{w_1.w_2}{T}$, $\frac{w_1.w_2(w_1-w_2)}{T}$, and $\frac{w_1.w_2(w_1-w_2)^2}{T}$.

2.3.4. The MRS model

MRS equation is written as Eq. (5):

$$\ln x_m = \beta_1 w_1' + \beta_2 w_2' + \beta_3\left(\frac{1}{w_1'}\right) + \beta_4\left(\frac{1}{w_2'}\right) + \beta_5 w_1' w_2' \quad (5)$$

β_1–β_5 are equation parameters and w_1' and w_2' are obtained by utilizing $w_1' = 0.96$ and $w_1 + 0.02$ and $w_2' = 0.96w_1 + 0.02$ [18].

2.4. Thermodynamic parameters

The thermodynamic properties of deferiprone (*i.e.,* the apparent standard dissolution Gibbs energy (ΔG°), standard dissolution enthalpy (ΔH°) and standard dissolution entropy change (ΔS°)) are calculated according to the Gibbs and van't Hoff equations. The modified van't Hoff equation can be written as Eq. (6):

$$\frac{\partial \ln x}{\partial\left(\frac{1}{T}-\frac{1}{T_m}\right)_p}=-\frac{\Delta H^{\circ}}{R} \tag{6}$$

x is the mole fraction solubility of deferiprone in the solvent mixtures, T is the absolute temperature (K) and R is the ideal gas constant (8.314 J $mol^{-1}{\cdot}K^{-1}$), respectively [19]. T_{hm} is the mean harmonic temperature and obtained by $T_{hm} = n / \sum_{i=1}^{n}(1/T)$, in which n is the number of set temperatures. ΔG° and ΔH° of solutions are calculated using the intercept and the slope of the plot of ln x against $1/T - 1/T_{hm}$, respectively, and the Gibbs equation is utilized to calculate ΔS°.

The relative contributions of entropy (ζ_{TS}) and enthalpy (ζ_H) to ΔG° of the deferiprone dissolution process are achieved using the following equations (Eqs. (7) and (8)) [20].

$$\zeta_H=\frac{|\Delta H^{\circ}|}{(|\Delta H^{\circ}|+|T\Delta S^{\circ}|)} \tag{7}$$

$$\zeta_{TS}=\frac{|T\Delta S^{\circ}|}{(|\Delta H^{\circ}|+|T\Delta S^{\circ}|)} \tag{8}$$

3. Results and discussion

3.1. Solubility profile of deferiprone and data modeling

Mole fraction solubility of deferiprone in the non-aqueous binary mixtures of propylene glycol and 2-propanol was investigated at the temperature range of 293.2–313.2 K by the shake-flask method. As can be observed from Table 2, the solubility of deferiprone (in mole fraction unit) was enhanced accompanied by the temperature increase in neat solvents and all studied solvent mixtures and the solubility values enhances with an increase in the mass ratio of propylene glycol, reached its highest value at $w_1 = 0.9$ and fell dramatically with further addition of propylene glycol. This observation showed that a binary solvent mixture with a mass fraction of 0.9 of propylene glycol provides a better solubilization environment for deferiprone. Interactions like hydrogen bonding and dipole-dipole between each solvent in a binary solvent mixture would generate an unmatchable environment for the solvent systems; so that the formation of a mutual hydrogen bond network between the alcoholic solvents plays a crucial role in the generation of synergistic solvation. The maximum solubility of deferiprone was observed at a specific ratio of solvents ($w_1 = 0.9$), maybe due to the high hydrogen bond network between propylene glycol molecules in a mass fraction of 1.0 (neat propylene glycol). However, such conditions is a combination of different factors such as polarity, van der Waals forces, preferential solvation, molecular shape and size, and other features of solute and solvent.

Experimental deferiprone solubility values in the non-aqueous binary mixtures of propylene glycol and 2-propanol were fitted through four mathematical cosolvency (the van't Hoff, the MRS, the Jouyban-Acree and Jouyban-Acree-van't Hoff) models and the *MRD*% values of the back-calculated solubility data were computed and along with the corresponding model parameters were shown in Tables 3–5. By comparison of the *MRD*% values, it was concluded that the van't Hoff model has the potential to provide a better correlation (2.0%). *MRD*% values of back-calculated solubility data by the MRS, the Jouyban-Acree, and Jouyban-Acree-van't Hoff models were 2.6, 3.1, and 1.3%, respectively, which confirmed their high ability for the solubility prediction. The main advantage of the Jouyban-Acree and Jouyban-Acree-van't Hoff models was the fitting of all solubility data in one step and generating one equation

Table 2
Experimental mole fraction solubility ($x_{m,T}$) values as the mean of three experiments (± standard deviation) measured for deferiprone in the binary mixtures of propylene glycol and 2-propanol at different temperatures.

w_1[a]	293.2 K	298.2 K	303.2 K	308.2 K	313.2 K
0.00	9.13 (±0.09) × 10^{-4}	1.05 (±0.02) × 10^{-3}	1.14 (±0.04) × 10^{-3}	1.30 (±0.08) × 10^{-3}	1.47 (±0.10) × 10^{-3}
0.10	1.05 (±0.05) × 10^{-3}	1.32 (±0.02) × 10^{-3}	1.55 (±0.05) × 10^{-3}	1.72 (±0.20) × 10^{-3}	1.91 (±0.24) × 10^{-3}
0.20	1.35 (±0.08) × 10^{-3}	1.66 (±0.03) × 10^{-3}	1.92 (±0.07) × 10^{-3}	2.20 (±0.08) × 10^{-3}	2.48 (±0.28) × 10^{-3}
0.30	1.75 (±0.04) × 10^{-3}	1.97 (±0.07) × 10^{-3}	2.36 (±0.18) × 10^{-3}	2.72 (±0.31) × 10^{-3}	3.15 (±0.08) × 10^{-3}
0.40	2.25 (±0.22) × 10^{-3}	2.48 (±0.19) × 10^{-3}	2.85 (±0.05) × 10^{-3}	3.12 (±0.10) × 10^{-3}	3.73 (±0.08) × 10^{-3}
0.50	2.48 (±0.05) × 10^{-3}	2.88 (±0.07) × 10^{-3}	3.22 (±0.14) × 10^{-3}	3.60 (±0.15) × 10^{-3}	4.32 (±0.15) × 10^{-3}
0.60	2.93 (±0.05) × 10^{-3}	3.30 (±0.17) × 10^{-3}	3.73 (±0.11) × 10^{-3}	4.10 (±0.48) × 10^{-3}	4.81 (±0.17) × 10^{-3}
0.70	3.26 (±0.05) × 10^{-3}	3.69 (±0.12) × 10^{-3}	4.12 (±0.14) × 10^{-3}	4.62 (±0.20) × 10^{-3}	5.61 (±0.19) × 10^{-3}
0.80	3.53 (±0.08) × 10^{-3}	4.06 (±0.08) × 10^{-3}	4.52 (±0.14) × 10^{-3}	5.11 (±0.09) × 10^{-3}	6.49 (±0.15) × 10^{-3}
0.90	3.78 (±0.10) × 10^{-3}	4.44 (±0.03) × 10^{-3}	5.05 (±0.34) × 10^{-3}	5.60 (±0.13) × 10^{-3}	7.07 (±0.26) × 10^{-3}
1.00	3.44 (±0.17) × 10^{-3}	4.03 (±0.05) × 10^{-3}	4.65 (±0.44) × 10^{-3}	5.44 (±0.19) × 10^{-3}	7.13 (±0.28) × 10^{-3}

[a] w_1 is mass fraction of propylene glycol in the propylene glycol and 2-propanol mixtures in the absence of deferiprone.

Table 3
The van't Hoff model parameters and the corresponding *MRD*% for deferiprone in the binary mixtures of propylene glycol and 2-propanol.

w_1	A	B	*MRD*%
0.00	0.304	−2140.835	1.0
0.10	2.368	−2692.550	3.0
0.20	2.818	−2756.115	1.8
0.30	3.017	−2750.369	1.0
0.40	1.642	−2274.444	1.9
0.50	2.340	−2445.993	1.6
0.60	1.723	−2217.380	1.1
0.70	2.450	−2401.860	2.2
0.80	3.379	−2652.341	3.2
0.90	3.699	−2722.128	2.4
1.00	5.284	−3220.343	3.3
Overall			2.0

Table 4
Parameters calculated for the Jouyban-Acree, and Jouyban-Acree-van't Hoff model for deferiprone solubility in the binary mixtures of propylene glycol and 2-propanol.

	Jouyban-Acree		Jouyban-Acree-van't Hoff	
Propylene glycol + 2-propanol	J_0	393.502	A_1	5.284
	J_1	84.110	B_1	−3220.343
	J_2	137.092	A_2	0.304
			B_2	−2140.835
			J_0	393.626
			J_1	83.984
			J_2	137.403
MRD%	2.6		3.1	

Table 5
The MRS model constants at investigated temperatures and the *MRD*% for back-calculated deferiprone solubility in the binary mixtures of propylene glycol and 2-propanol.

T (K)	β_1	β_2	β_3	β_4	β_5	*MRD*%
293.2	−5.564	−7.262	0.004	−0.002	1.755	1.4
298.2	−5.315	−6.914	0[a]	−0.004	1.051	0.9
303.2	−5.205	−6.716	−0.002	−0.003	0.964	1.0
308.2	−5.106	−6.592	−0.002	−0.002	0.957	1.1
313.2	−4.918	−6.568	0[a]	0[a]	1.235	2.1
Overall *MRD*%						1.3

[a] Not statistically significant (p-value >0.05).

for back-calculating/predicting of solubility data in different solvent compositions at various temperatures. However, for other models and depending on the functionality to composition or temperature, several models need to be used for solubility prediction in a known temperature or solvent composition. Aside from correlative ability, the predictability power of the Jouyban-Acree-van't Hoff model was also investigated by training the model with the minimum data points. The selected data points for training were solubility data in

Table 6
Measured density (g·cm^{-3}) of deferiprone saturated solutions in the binary mixtures of propylene glycol and 2-propanol at different temperatures.

w_1	293.2 K	298.2 K	303.2 K	308.2 K	313.2 K
0.00	0.781 ± 0.001	0.778 ± 0.001	0.777 ± 0.001	0.774 ± 0.001	0.772 ± 0.001
0.10	0.803 ± 0.001	0.801 ± 0.001	0.798 ± 0.001	0.794 ± 0.001	0.794 ± 0.001
0.20	0.822 ± 0.001	0.821 ± 0.001	0.819 ± 0.001	0.817 ± 0.001	0.817 ± 0.001
0.30	0.848 ± 0.001	0.843 ± 0.001	0.842 ± 0.001	0.840 ± 0.001	0.840 ± 0.001
0.40	0.871 ± 0.001	0.868 ± 0.001	0.868 ± 0.001	0.867 ± 0.001	0.866 ± 0.001
0.50	0.895 ± 0.001	0.893 ± 0.001	0.892 ± 0.001	0.890 ± 0.001	0.889 ± 0.001
0.60	0.923 ± 0.001	0.921 ± 0.001	0.918 ± 0.001	0.917 ± 0.001	0.913 ± 0.001
0.70	0.949 ± 0.001	0.946 ± 0.001	0.945 ± 0.001	0.945 ± 0.001	0.945 ± 0.001
0.80	0.976 ± 0.001	0.973 ± 0.001	0.972 ± 0.001	0.971 ± 0.001	0.970 ± 0.001
0.90	1.005 ± 0.001	1.001 ± 0.001	1.002 ± 0.001	0.999 ± 0.001	0.999 ± 0.001
1.00	1.035 ± 0.001	1.031 ± 0.001	1.032 ± 0.001	1.030 ± 0.001	1.028 ± 0.001

neat solvents at 293.2 and 313.2 K and propylene glycol mass fractions of 0.3, 0.5, and 0.7. The *MRD*% values for predicted data were 3.9, 2.0, 4.1, 6.1, and 3.0, respectively.

In addition to solubility data, the density ($g{\cdot}cm^{-3}$) of deferiprone saturated mixtures in the non-aqueous binary mixtures of propylene glycol and 2-propanol at different temperatures were also measured by using a pycnometer and reported in Table 6. For the mathematical representation of density data, they were correlated to the Jouyban-Acree model and the trained model is as Eq. (9) [21]:

$$\ln \rho_{m,T} = w_1 \ln \rho_{1,T} + w_2 \ln \rho_{2,T} - 2.901\frac{w_1.w_2}{T}_{+1.779}\frac{w_1.w_2(w_1 - w_2)}{T} \quad (9)$$

The *MRD*% for back-calculated data was 0.1% which confirmed the high ability of the Jouyban-Acree model for the prediction of other physicochemical properties such as density.

3.2. Calculation of thermodynamic parameters of deferiprone dissolution

Based on the equilibrium data, the apparent thermodynamic properties of the deferiprone dissolution (ΔG°, ΔH°, and ΔS°) were estimated using the Gibbs and modified van't Hoff equations at $T_{hm} = 303.0$ K and displayed in Table 7. The thermodynamic properties of the dissolution process were all positive values, indicating that the dissolution of deferiprone in the chosen solvents was endothermic and entropy-driven. Moreover, ΔG° values were in the range of 13.31 and 17.03 kJ mol^{-1} with the lowest value at $w_1 = 0.9$, demonstrating that the deferiprone dissolution procedure was more favorable in the mixtures with the highest solubility.

An enthalpy-entropy compensation analysis was employed to study the main mechanisms involved in the cosolvent action. As shown in Fig. 2, deferiprone mass transfer exhibits a non-linear trend with a negative slope from $0.0 \leq w_1 \leq 0.3$, $0.4 \leq w_1 \leq 0.5$, and $0.6 \leq w_1 \leq 1.0$ and a positive slope from $0.3 \leq w_1 \leq 0.4$, and $0.5 \leq w_1 \leq 0.6$. In the first case, the driving mechanism for the transfer of deferiprone was entropy, whereas, in the latter, the driving mechanism was enthalpy.

The Kamlet-Abboud-Taft Linear Solvation Energy Relationship (KAT-LSER) model is also applied here for the experimental solubility values of deferiprone (compound 3) to explain the Lewis-acid-base and polarization effects of {propylene glycol (compound 1) + isopropanol (compound 2)} mixtures upon the improvement of this physicochemical property. Classical KAT-LSER model takes the form of Eq. (10) [22–24].

$$\ln x_3 = c_0 + c_1\alpha_{1+2} + c_2\beta_{1+2} + c_3\pi_{1+2} + c_4\left(\frac{V_3\delta^1_{1+2}}{100RT}\right) \quad (10)$$

where,$c_1\alpha_{1+2}$ and $c_2\beta_{1+2}$ refer to the energetic terms associated with specific solute–solvent Lewis acid and base interactions, respectively; $c_3\pi_{1+2}$ represents the energetic term related to non-specific interactions, whereas the last term in Eq. (10) denotes the cavity term, which defines the energetic requirement for solvent–solvent interactions. The last term designates the deferiprone accommodation energy as a product of the Hildebrand solubility parameter of the solvent mixture (δ_{1+2}) and the molar volume of deferiprone (V_3). V3 is assumed to be calculated using the Fedors method, namely 106.4 cm^3 mol^{-1} [25]. The universal gas constant (R = 8.3145 J $mol^{-1}{\cdot}K^{-1}$) and experimental temperature (T/K) are considered in the denominator to obtain a dimensionless magnitude for the cavity term. c_0 represents the deferiprone–deferiprone interactions and measures the intercept when $\alpha_{1+2} = \beta_{1+2} = \underline{\pi}_{1+2} = \delta_{1+2} = 0$. c_1 and c_2 are a measure of the susceptibility of deferiprone to drug–solvent interactions of specific hydrogen bonding, while c_3 and c_4 represent the solute sensitivity to the nonspecific electrostatic deferiprone–solvent and solvent–solvent interactions. Table 8 summarizes the logarithmic solubilities of deferiprone as well as the calculated solvatochromic parameters of the solvent mixtures assuming additive volume behavior from individual values for neat solvents as reported in the literature [26,27]. In this way, the KAT-LSER model obtained is shown as Eq. (11) (with $n = 11$, $r^2 = 0.998$, and $F = 1926$).

$$\ln x_3 = -11.69 + 54.12\pi_{1+2} + 89.21\left(\frac{V_3\delta^2_{1+2}}{100RT}\right) \quad (11)$$

As observed, c_1 and c_2 were equal to 0, indicating that Lewis acid-base effects are compensated with deferiprone in the mixtures of these alcohols. Otherwise, the positive value of c_3 (54.12) demonstrates the favorable contribution of polarizability behavior on the deferiprone solubility. Otherwise, the negative values of c_0 (−11.69) and c_4 (−89.21) demonstrate the unfavorable contribution of deferiprone-deferiprone interactions and cavity energy requirements on the solubility of this drug. Moreover, if the absolute values of c_1 and c_4 are compared together the following contribution percentages are obtained: (38.8 and 62.2) %, respectively. Thus, cavity effects make a higher unfavorable contribution to drug dissolution.

4. Conclusions

The results of the current work showed that deferiprone solubility increased with temperature increasing for all mixtures. In the binary mixture compositions, the solubility of deferiprone increased with increase in propylene glycol mass fraction in the range of w_1 = 0.0 to 0.9 and the highest deferiprone solubility was obtained in $w_1 = 0.9$. In the mathematical representation of the solubility data, the *MRDs%* of the fitting by the van't Hoff, the Jouyban-Acree and Jouyban-Acree-van't Hoff, and the MRS models were 2.0, 2.6, 3.1, and 1.3% demonstrating that the relevant results have potential to provide a basic model for the prediction of the deferiprone solubilization.

Table 7
Apparent thermodynamic parameters for dissolution behavior of deferiprone in the binary mixtures of propylene glycol and 2-propanol at T_{hm}.

w_1	ΔG° (kJ·mol^{-1})	ΔH° (kJ·mol^{-1})	ΔS° (J·K^{-1}·mol^{-1})	$T\Delta S^\circ$ (kJ·mol^{-1})	ζH	ζTS
0.00	17.03	17.83	2.64	0.80	0.957	0.043
0.10	16.42	22.36	19.62	5.94	0.790	0.210
0.20	15.81	22.82	23.13	7.01	0.765	0.235
0.30	15.27	22.81	24.89	7.54	0.752	0.248
0.40	14.77	18.86	13.49	4.09	0.822	0.178
0.50	14.44	20.30	19.34	5.86	0.776	0.224
0.60	14.09	18.40	14.23	4.31	0.810	0.190
0.70	13.80	19.97	20.38	6.17	0.764	0.236
0.80	13.54	22.07	28.15	8.53	0.721	0.279
0.90	13.31	22.62	30.74	9.31	0.708	0.292
1.00	13.46	26.81	44.04	13.34	0.668	0.332

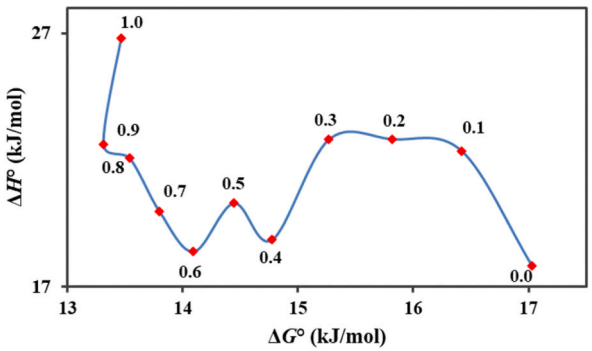

Fig. 2. Enthalpy-entropy compensation plot for deferiprone in the mixtures of propylene glycol and 2-propanol at 303.0 K. The points represent the mass fraction of propylene glycol in propylene glycol and 2-propanol mixtures in the absence of deferiprone.

Table 8
Logarithmic mole fraction solubility of deferiprone and solvatochromic parameters of solvent mixtures at 298.2 K.

w_1	$\ln x_3$	α_{1+2}	β_{1+2}	π_{1+2}	$\left(\frac{V_3\delta_{1+2}^2}{100RT}\right)$
0.00	−6.862	0.760	0.840	0.480	0.237
0.10	−6.631	0.765	0.835	0.502	0.248
0.20	−6.399	0.771	0.830	0.525	0.259
0.30	−6.228	0.777	0.825	0.549	0.271
0.40	−5.999	0.783	0.820	0.574	0.285
0.50	−5.849	0.790	0.814	0.601	0.299
0.60	−5.712	0.797	0.808	0.629	0.314
0.70	−5.603	0.805	0.802	0.659	0.331
0.80	−5.506	0.813	0.795	0.690	0.350
0.90	−5.417	0.821	0.788	0.724	0.370
1.00	−5.515	0.830	0.780	0.760	0.391

Author contribution statement

Homa Rezaei: Performed the experiments; Wrote the paper.
Elaheh Rahimpour: Conceived and designed the experiments; Analyzed and interpreted the data.
Fleming Martinez: Analyzed and interpreted the data.
Abolghasem Jouyban: Contributed reagents, materials, analysis tools or data.

Funding statement

Abolghasem Jouyban was supported by Tabriz University of Medical Sciences [69212].

Data availability statement

Data will be made available on request.

Declaration of competing interest

The authors declare that they have no known competing financial interests or personal relationships that could have appeared to influence the work reported in this paper

Acknowledgments

The research protocol was approved and supported by the Student Research Committee under grant number 69212 Faculty of Pharmacy, Tabriz University of Medical Sciences, Tabriz, Iran.

References

[1] M. Zurlo, P. De Stefano, C. Borgna-Pignatti, A. Di Palma, C. Melevendi, A. Piga, F. Di Gregorio, M. Burattini, S. Terzoli, Survival and causes of death in thalassaemia major, Lancet 334 (1989) 27–30, https://doi.org/10.1016/s0140-6736(89)90264-x.
[2] V. Viprakasit, V. Tanphaichitr, C. Mahasandana, A. Assteerawatt, L. Suwantol, G. Veerakul, S. Kankirawatana, P. Pung-Amritt, V. Suvatte, Linear growth in homozygous beta-thalassemia and beta-thalassemia/hemoglobin E patients under different treatment regimens, J. Med. Assoc. Thai. 84 (2001) 929–941.
[3] A. Chuansumrit, D. Songdej, N. Sirachainan, P. Wongwerawattanakoon, P. Kadegasem, W. Sasanakul, Safety profile of a liquid formulation of deferiprone in young children with transfusion-induced iron overload: a 1-year experience, Paediatr. Int. Child Health 36 (2016) 209–213, https://doi.org/10.1179/2046905515Y.0000000040.
[4] J. Porter, V. Viprakasit, A. Kattamis, Guidelines for the Management of Transfusion Dependent Thalassaemia (TDT), third ed., Thalassaemia International Federation, 2014 [Internet].
[5] N.T. Tran, B. Akkawat, N.P. Morales, P. Rojnuckarin, R. Luechapudiporn, Antiplatelet activity of deferiprone through cyclooxygenase-1 inhibition, Platelets 31 (2020) 505–512, https://doi.org/10.1080/09537104.2019.1648782.
[6] M. El Alfy, T.T. Sari, C.L. Lee, F. Tricta, A. El-Beshlawy, The safety, tolerability, and efficacy of a liquid formulation of deferiprone in young children with transfusional iron overload, J. Pediatr. Hematol. Oncol. 32 (2010) 601–605, https://doi.org/10.1097/MPH.0b013e3181ec0f13.
[7] P. Augustijns, M.E. Brewster, Solvent Systems and Their Selection in Pharmaceutics and Biopharmaceutics, Springer, New York, 2007.
[8] V.H. Thomas, S. Bhattachar, L. Hitchingham, P. Zocharski, M. Naath, N. Surendran, C.L. Stoner, A. El-Kattan, The road map to oral bioavailability: an industrial perspective, Expet Opin. Drug Metabol. Toxicol. 2 (2006) 591–608, https://doi.org/10.1517/17425255.2.4.591.
[9] E.H. Kerns, High throughput physicochemical profiling for drug discovery, J. Pharm. Sci. 90 (2001) 1838–1858, https://doi.org/10.1002/jps.1134.
[10] A. Jouyban-Gharamaleki, L. Valaee, M. Barzegar-Jalali, B. Clark, W. Acree Jr., Comparison of various cosolvency models for calculating solute solubility in water–cosolvent mixtures, Int. J. Pharm. 177 (1999) 93–101, https://doi.org/10.1016/S0378-5173(98)00333-0.
[11] A. Jouyban, Review of the cosolvency models for predicting solubility of drugs in water-cosolvent mixtures, J. Pharm. Pharmaceut. Sci. 11 (2008) 32–58, https://doi.org/10.18433/J3PP4K.
[12] M. Abbasi, F. Martinez, A. Jouyban, Prediction of deferiprone solubility in aqueous mixtures of ethylene glycol, propylene glycol and polyethylene glycol 400 at various temperatures, J. Mol. Liq. 197 (2014) 171–175, https://doi.org/10.1016/j.molliq.2014.05.004.
[13] A. Fathi-Azarbayjani, M. Abbasi, J. Vaez-Gharamaleki, A. Jouyban, Measurement and correlation of deferiprone solubility: investigation of solubility parameter and application of van't Hoff equation and Jouyban–Acree model, J. Mol. Liq. 215 (2016) 339–344, https://doi.org/10.1016/j.molliq.2015.12.005.
[14] A. Jouyban, M. Abbasi, E. Rahimpour, M. Barzegar-Jalali, J. Vaez-Gharamaleki, Deferiprone solubility in some non-aqueous mono-solvents at different temperatures: experimental data and thermodynamic modelling, Phys. Chem. Liq. 56 (2018) 619–626, https://doi.org/10.1080/00319104.2017.1368079.
[15] A. Jouyban, M.A. Fakhree, in: W.E. Acree (Ed.), Experimental and Computational Methods Pertaining to Drug Solubility, Toxicity and Drug Testing, IntechOpen, 2012, pp. 187–218.
[16] C. Zhou, X. Shi, H. Wang, N. An, Measurement and correlation of solubilities of trans-ferulic acid in solvents, J. Chem. Ind. Eng. 58 (2007) 2705.
[17] A. Jouyban, W.E. Acree Jr., Mathematical derivation of the Jouyban-Acree model to represent solute solubility data in mixed solvents at various temperatures, J. Mol. Liq. 256 (2018) 541–547, https://doi.org/10.1016/j.molliq.2018.01.171.
[18] A.B. Ochsner, R.J. Belloto Jr., T.D. Sokoloski, Prediction of xanthine solubilities using statistical techniques, J. Pharm. Sci. 74 (1985) 132–135.
[19] S. Vahdati, A. Shayanfar, J. Hanaee, F. Martínez, W.E. Acree Jr., A. Jouyban, Solubility of carvedilol in ethanol+ propylene glycol mixtures at various temperatures, Ind. Eng. Chem. Res. 52 (2013) 16630–16636, https://doi.org/10.1021/ie403054z.
[20] G.L. Perlovich, S.V. Kurkov, A. Bauer-Brandl, Thermodynamics of solutions: II. Flurbiprofen and diflunisal as models for studying solvation of drug substances, Eur. J. Pharmaceut. Sci. 19 (2003) 423–432, https://doi.org/10.1016/S0928-0987(03)00145-3.
[21] A. Jouyban, W.E. Acree Jr., A single model to represent physico-chemical properties of liquid mixtures at various temperatures, J. Mol. Liq. 323 (2021), 115054, https://doi.org/10.1016/j.molliq.2020.115054.
[22] W.X. Li, A. Farajtabar, N. Wang, Z.T. Liu, Z.H. Fei, H.K. Zhao, Solubility of chloroxine in aqueous co-solvent mixtures of N, N-dimethylformamide, dimethyl sulfoxide, N-methyl-2-pyrrolidone and 1,4-dioxane: determination, solvent effect and preferential solvation analysis, J. Chem. Thermodyn. 138 (2019) 288–296, https://doi.org/10.1016/j.jct.2019.07.001.
[23] Y. Li, C. Li, X. Gao, H. Lv, Equilibrium solubility, preferential solvation and solvent effect study of clotrimazole in several aqueous co-solvent solutions, J. Chem. Thermodyn. 151 (2020), 106255, https://doi.org/10.1016/j.jct.2020.106255.
[24] Y. Cong, C. Du, K. Xing, Y. Bian, X. Li, M. Wang, Investigation on co-solvency, solvent effect, Hansen solubility parameter and preferential solvation of fenbufen dissolution and models correlation, J. Mol. Liq. 348 (2022), 118415, https://doi.org/10.1016/j.molliq.2021.118415.
[25] R.F. Fedors, A method for estimating both the solubility parameters and molar volumes of liquids, Polym. Eng. Sci. 14 (1974) 147–154, https://doi.org/10.1002/pen.760140211.
[26] A.F.M. Barton, Handbook of Solubility Parameters and Other Cohesion Parameters, second ed., CRC Press, New York, 1991.
[27] Y. Marcus, The Properties of Solvents, John Wiley & Sons, Chichester, 1998.